Appl Phys B (2009) 95: 351–359
DOI 10.1007/s00340-009-3373-7

Applied Physics B
Lasers and Optics

Tailor-made metal nanoparticles as SERS substrates

F. Hubenthal · D. Blázquez Sánchez · N. Borg · H. Schmidt · H.-D. Kronfeldt · F. Träger

Received: 14 October 2008 / Revised version: 15 January 2009 / Published online: 13 February 2009

Abstract In this contribution we summarize recent experiments with the objective to generate optimized substrates for surface-enhanced Raman spectroscopy (SERS). For this purpose, the well-established laser-assisted growth technique has been applied, which relies on a precise control of the growth kinetics of supported metal nanoparticles. With this method reproducible and stable SERS substrates with tailor-made optical properties possing best field enhancements were produced for specific excitation wavelengths and detection ranges. Optimization of the SERS substrates has been achieved by stabilizing the localized surface plasmon polariton resonance (SPR) of gold nanoparticles in the vicinity of the laser wavelength of $\lambda = 647$ nm and $\lambda = 785$ nm used for SERS excitation. After nanoparticle preparation, SERS spectra of pyrene were obtained using naturally grown nanoparticles and nanoparticles prepared by laser-assisted growth.

The most important result is that the optimized substrates prepared by laser-assisted growth exhibit a significantly higher signal-to-noise ratio as compared to naturally grown nanoparticles. They are even better than substrates whose SPR has been tuned to the excitation wavelength by an elevated temperature during preparation. Another important observation is that all SERS spectra exhibit excellent reproducibility and the substrates do not show degradation during the measurements. Finally, the SERS enhancement factors due to the optimized substrates have been estimated and are on the order of 10^5 to 10^6.

PACS 78.30.-j · 73.20.Mf · 42.62.Fi · 71.45.Gm · 78.67.Bf · 73.22.Lp

1 Introduction

Noble metal nanoparticles have found an increasing interest in recent years. One reason is the unique optical properties of noble metal nanoparticles (NPs), which are dominated by localized surface plasmon polaritons resonances (SPRs), i.e., collective oscillations of the conduction band electrons. Associated with the excitation of an SPR is a local field enhancement in the vicinity of the particle surface. The latter effect is the basis of all surface-enhanced spectroscopies and has been used, for example, in surface-enhanced Raman spectroscopy [1–9], surface-enhanced fluorescence [10, 11], or confocal microscopy [12].

Raman scattering, for example, is a vibrational spectroscopic technique that allows substance identification due to its inherent molecule fingerprinting capability, by detecting the inelastic scattered laser light from molecules. The main drawback of Raman spectroscopy is the small fraction of inelastically scattered light, which is on the order of 10^{-6}. This can be overcome by surface-enhanced Raman spectroscopy (SERS). If the incident laser light excites a surface plasmon polariton resonance in the metal nanostructure, a strong field enhancement in the vicinity of its surface can be generated. Thus, the metal structure acts as an antenna that does not only enhance the incident laser field but also the Raman scattered field [13, 14]. Since its discovery, SERS has

F. Hubenthal (✉) · D. Blázquez Sánchez · N. Borg · F. Träger
Institut für Physik and Center for Interdisciplinary Nanostructure Science and Technology—CINSaT, Universität Kassel, Heinrich-Plett-Str. 40, 34132 Kassel, Germany
e-mail: hubentha@physik.uni-kassel.de

H. Schmidt · H.-D. Kronfeldt
Institute of Optics and Atomic Physics, Technical University Berlin, Hardenbergstrasse 36, 10623 Berlin, Germany

been increasingly exploited, opening up exciting opportunities in the field of biophysical and biomedical spectroscopy. It has even been demonstrated that under certain circumstances the sensitivity of Raman spectroscopy can be improved so that single molecules are detectable [1, 2, 7, 15]. As a spectroscopic tool, SERS has the potential to combine the sensitivity of fluorescence with the structural information of Raman spectroscopy [7].

The field enhancement factor f_{Field} is defined by $f_{\mathrm{Field}} = \frac{E_{\mathrm{Loc}}}{E_{\mathrm{In}}}$, where $E_{\mathrm{Loc}} = E_{\mathrm{In}} + E_{\mathrm{Struc}}$ is the local field at the point of investigation, E_{In} is the incoming light field, and E_{Struc} is the field of the nanostructure due to the excitation of an SPR. A molecule in the vicinity of such a metal nanostructure feels the local field E_{Loc}, and under ideal conditions, the SERS-signal can be enhanced up to 10^{12} to 10^{13} [1, 2, 16, 17]. It has been demonstrated that best SERS enhancement factors f_{SERS} can be obtained if the SPR is in the vicinity of the excitation wavelength [18, 19], since f_{SERS} for spherical nanoparticles is

$$f_{\mathrm{SERS}} \propto \left(f_{\mathrm{Field}}^{\mathrm{Exc}}\right)^2 \cdot \left(f_{\mathrm{Field}}^{\mathrm{Signal}}\right)^2 \cdot f_{\mathrm{Chem}} \cdot \left(\frac{R}{R+d}\right)^{12}, \qquad (1)$$

where $(f_{\mathrm{Field}}^{\mathrm{Exc}})$ is the field enhancement at the excitation wavelength, $(f_{\mathrm{Field}}^{\mathrm{Signal}})$ is the field enhancement at the Raman scattered light, f_{Chem} is the chemical enhancement, R the radius of the particle, and d is the distance between the nanoparticle surface and the molecule. While the contribution of the chemical enhancement is on the order of 10 to 10^2 [15, 20] and plays only a minor role for f_{SERS}, the main contribution originates from the electromagnetic enhancement. However, the field enhancement f_{Field} of the nanoparticles depends critically on their size and shape. Hence, reliable fabrication methods that produce particles with homogeneous sizes and shapes are highly desired to provide substrates with an optimum enhancement of the Raman signal of adsorbed molecules. For this purpose, standard lithography techniques [18] or nanosphere lithography has been used [19]. Another very versatile possibility is tailoring of nanoparticles with laser light, which found great interest and use in recent years [21–24]. In particular, it has been shown that tailoring of supported nanoparticles with laser light allows fabrication of nanoparticle ensembles with tunable plasmon resonances and narrow size distributions.

In this contribution we demonstrate that metal nanoparticles prepared by laser-assisted growth [21, 25] can be exploited to generate stable and highly reproducible nanoparticle ensembles designed for certain molecule/laser excitation wavelength combinations. By tailoring the shape of the nanoparticles during nanoparticle growth with laser light, stabilization of the SPR at a certain predetermined energetic position can be achieved. The improvement of the Raman signal due to the tailored nanoparticles will be demonstrated.

2 Experimental

2.1 Nanoparticle growth and characterization

Gold nanoparticles were produced by deposition with subsequent diffusion and nucleation of thermal gold atoms, i.e., Volmer–Weber growth [26]. The growth kinetic generates oblate nanoparticles [25], whose shape is characterized by the axial ratio a/b, where a denotes the short axis perpendicular, and b the long axis parallel to the substrate surface. The size of the nanoparticles is determined by the equivalent radius R_{eq}, which is the radius of a sphere with the same volume as the actual particles. Due to the self-organized growth process, nanoparticle ensembles with a size and shape distribution of below 40% [22, 27, 28] are obtained and the SPR is inhomogeneously broadened [29–31].

For small nanoparticles with sizes between $R_{\mathrm{eq}} = 1$ nm to $R_{\mathrm{eq}} = 20$ nm, the positions of the SPR modes depend only on the axial ratio and not on the particle size [32, 33]. In addition, if the distance between the nanoparticles is large compared to their radius, particle–particle interaction does not play a role [34]. Hence, theoretical modeling of the position of the SPR using the quasistatic dipole approximation is sufficient to extract the axial ratio of the particles [33]. To determine the average nanoparticle size, the number density of the nanoparticles on the substrate was measured by noncontact atomic force microscopy. Together with the deposited amount of material, which was measured with the microbalance, we can calculate the average volume, i.e., the average equivalent radius of the nanoparticles $\langle R_{\mathrm{eq}} \rangle$ [25].

2.2 Experimental set-up

Preparation of gold nanoparticles was carried out under ultrahigh vacuum (UHV) conditions at room temperature. The pressure in the chamber used for preparation and in situ optical characterization of the nanoparticles was better than 10^{-8} mbar. For nanoparticle preparation, an electron beam evaporator (Omicron, EFM-3), equipped with a filter for removing charged particles was used. A beam of thermal gold atoms was generated, using a molybdenum crucible with a ceramic receptacle (GE Advanced Ceramics, Boralloy) carrying a small gold ingot. The atom flux was monitored by a quartz crystal microbalance (Inficon, 6 MHz, 008-010-G10) and set to $8 \times 10^{14} \frac{\mathrm{atoms}}{\mathrm{cm}^2 \cdot \mathrm{min}}$. Cylindrical sapphire plates (CrysTec, orientation (0001)) with a diameter of 10 mm and a thickness of 0.5 mm served as substrates.

The light of a Xe-arc lamp (Osram, XBO 450 W/1) combined with a monochromator (AMKO, 1200 lines/mm, blaze: 250 nm) and a polarizer was used to measure the optical spectra under UHV conditions. The angle of incidence was set to 45°, and s-polarized light was used. The extinction signal was determined from the signals of two photodiodes, one in front of and a second one behind the sample.

The nanoparticles were further characterized by noncontact atomic force microscopy under ambient conditions (ThermoMicroscopes, Autoprobe CP).

For laser tailoring, the nanoparticles were irradiated in UHV at room temperature with nanosecond pulsed laser light generated by a BBO-MOPO (beta-barium borate master optical parametrical oscillator, Spectra Physics, Quanta-Ray MOPO-730), pumped by the third harmonic ($\lambda = 355$ nm, $h\nu = 3.49$ eV) of an Nd:YAG laser (Spectra Physics, Quanta-Ray Pro 230). The laser pulse duration was approximately 5 ns with a repetition rate of 10 Hz.

A micro Raman setup was employed to record the SERS spectra. Briefly, the 647.1 nm line of a krypton ion laser (Spectra Physics, Model 2020) was applied for excitation with 20 mW on the sample. The backscattered light was collected by means of an objective with a numerical aperture of 0.3, filtered with a notch plus filter (Kaiser) and analyzed by a spectrograph (Chromex 250 IS) equipped with a 600 mm^{-1} grating and a liquid–nitrogen cooled deep depletion CCD (Princeton Instruments, 400×1340 pixel). The setup had a spectral bandpass of 6 cm^{-1}. For the measurements, 2 µl of a 2 mM solution of pyrene (Fluka, purity >99%) in methanol (Merck, purity >99.5%) were spotted on the SERS substrates. After drying in air, the SERS response was optimized by adjusting the position of the substrate along the focal axis by means of a translation stage. Spectra were measured with 1 s integration time, and three accumulations were taken. Measurements with excitation at $\lambda = 785$ nm were performed with a similar set up using a 785 nm DFB-diode laser with 30 mW on the sample, a collection objective with numerical aperture of 0.2 and two Raman edge filters instead of the notch filter. The spectra were recorded with a spectrograph (PI 320 i) and a 1024×256 pixel liquid nitrogen cooled deep depletion CCD (PI). The set up had a bandpass of 10 cm^{-1}. Spectra were measured with 10 s integration time, and 40 accumulations were taken.

3 Laser assisted growth

The well-established method of laser-assisted growth [21–23, 35] has been applied to tailor the optical properties of gold nanoparticles with laser light. In brief, laser-assisted growth exploits the shape dependence of the spectral position of the (1,1)-mode of the SPR. If the nanoparticles grow undisturbed, there is a strong correlation between the shape and the size of the nanoparticles. While small nanoparticles are nearly spherical, their axial ratio drops off with increasing size. As a consequence, the (1,1)-mode of the plasmon resonance shifts to lower photon energies [21, 25]. Figure 1a depicts extinction spectra of naturally grown gold nanoparticles on sapphire for coverages between $\Theta = 0.8 \times 10^{16}$ atoms/cm^2 and $\Theta = 7.6 \times 10^{16}$ atoms/cm^2, i.e., increasing nanoparticle sizes. A clear shift of the SPR for increasing coverage is observed. In contrast, if the nanoparticles are irradiated with nanosecond-pulsed laser light with a photon energy below the energy of the SPR, the growth process can be drastically altered [21–23, 35]. As soon as the extinction profile of the SPR overlaps with the laser line, light absorption occurs. The absorption of laser light causes a temperature rise of the resonant nanoparticles, sufficiently high to stimulate self-diffusion and desorption of atoms from the edges and perimeters of the particles. Both effects lead to a reshaping of the nanoparticles towards more spherical objects. If appropriate preparation conditions are chosen, the decrease of the axial ratio due to particle growth competes with the influence of the irradiation with laser light and leads to a stabilization of the SPR at a certain predetermined position. Hence, laser-assisted growth is a self-regulating mechanism where the laser line acts as a barrier for the SPR and the chosen laser wavelength determines the final position of the SPR [21, 25]. Figure 1b shows the extinction spectra of gold nanoparticles prepared by laser-assisted growth, applying a fluence of $F = 60$ mJ/cm^2 and a photon energy of $h\nu = 1.27$ eV for different nominal coverage.[1] With these parameters, a stabilization of the SPR at a wavelength of $\lambda_{SPR} = 745$ nm has been achieved. We emphasize, that the spectra depicted in Fig. 1 were recorded in situ. Due to subsequent self diffusion of surface atoms, which takes place in the first 24 hours after preparation, the shape of the nanoparticles is altered and hence, the SPRs are shifted to their final positions of $\lambda_{SPR} = 655$ nm for the tailored and to $\lambda_{SPR} = 850$ nm for the naturally grown nanoparticles, respectively (cf. Fig. 2).

4 Results

For the SERS measurements, five gold nanoparticle ensembles have been prepared on sapphire substrates. Three samples (A1 to A3) have been prepared for an SERS excitation wavelength of $\lambda = 647$ nm and two samples (B1 and B2) for $\lambda = 785$ nm.

4.1 Excitation wavelength $\lambda = 647$ nm

The first set of experiments has been performed with an SERS excitation wavelength of $\lambda = 647$ nm. Sample A1

[1] The nominal coverage is the coverage without considering desorption of atoms. Due to heating of the nanoparticles, desorption may occur, and the actual coverage on the substrate might be less than the nominal coverage. However, the influence due to desorption of atoms on the coverage is small, because significant desorption has been observed only for fluences higher than $F = 75$ mJ/cm^2 [21, 36].

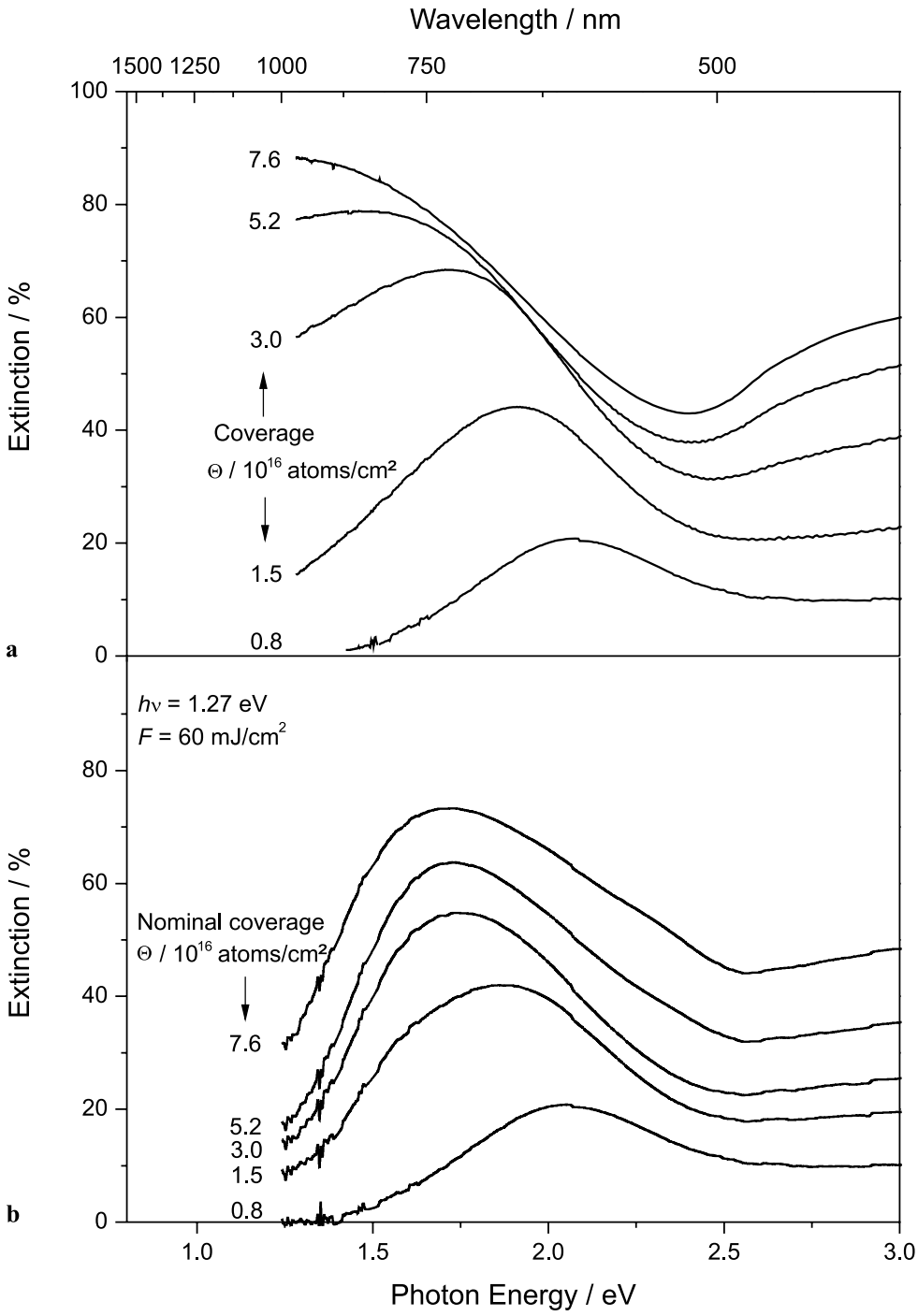

Fig. 1 Extinction spectra of gold nanoparticles for coverages between $\Theta = 0.8 \times 10^{16}$ atoms/cm^2 and $\Theta = 7.6 \times 10^{16}$ atoms/cm^2, corresponding to 5.3 and 50.1 equivalent monolayers of gold, respectively. 1 equivalent monolayer $= 1.517 \times 10^{15}$ atoms/cm^2 **a** Natural growth, **b** Laser-assisted growth, using a fluence of $F = 60$ mJ/cm^2 and a photon energy of $h\nu = 1.27$ eV

was prepared by natural growth, while for sample A2, laser-assisted growth has been applied, using a photon energy of the laser light of $h\nu = 1.27$ eV and a fluence of $F = 60$ mJ/cm^2 (cf. Fig. 1b). Sample A3 was also prepared by natural growth, but the substrate temperature was slightly increased during nanoparticle growth compared to samples A1 and A2. The higher temperature stimulates surface diffusion of atoms resulting in more spherical nanoparticles. Hence, the SPR of the nanoparticles can also be influenced by the substrate temperature, which, for sample A3, was chosen to be 350 K. As a result, the position of the SPR of sample A3 coincides with the SPR of sample A2. Thus, the SERS enhancement obtained from optimized nanoparticles tailored with laser light and obtained from the thermally altered nanoparticles due to elevated temperatures can be compared. In the following, samples A1, A2, and A3 are called naturally grown, laser-tailored, and thermally altered, respectively. Table 1 summarizes the

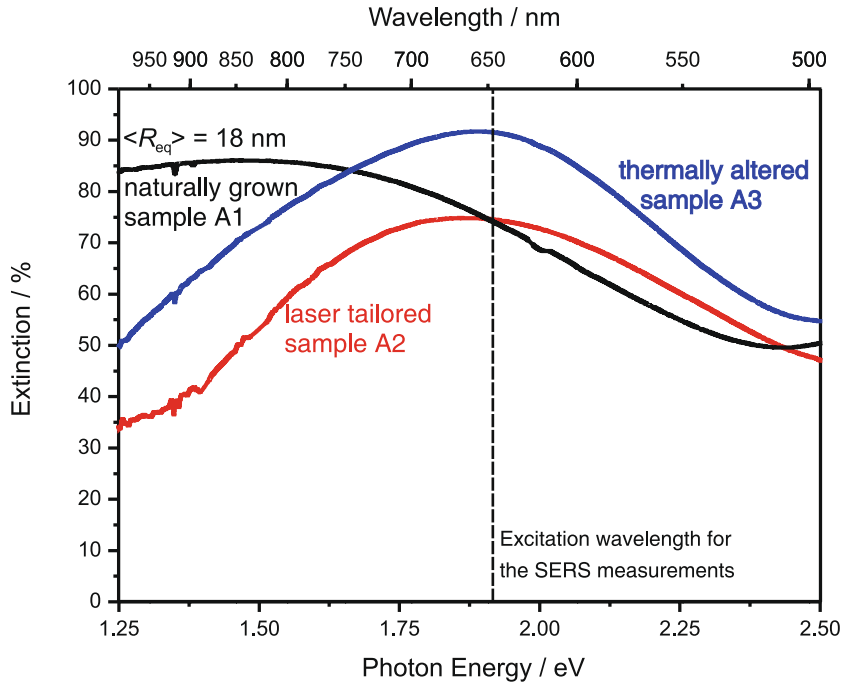

Fig. 2 Extinction spectra of samples A1 to A3

Table 1 Preparation parameters and characteristics of the SERS substrates A1 to A3 for an excitation with $\lambda = 647$ nm

	A1	A2	A3
$\Theta/10^{16}$ cm^{-2}	7.6 ± 0.8	7.6 ± 0.8	7.6 ± 0.8
$T_{support}/10^2$ K	3.0	3.0	3.5
$\langle a/b \rangle$	0.07	0.15	0.14
λ_{SPR}/nm	≈850	655	665

preparation parameters and the characteristics of the samples.

The mean radius of the nanoparticles and the nanoparticle density n_p for the ensemble prepared in natural growth amounts to $\langle R_{eq} \rangle = (18 \pm 3)$ nm and $n_p = (1.0 \pm 0.1) \times 10^{11}$ cm^{-2}, respectively. For the tailored nanoparticle ensemble and for the thermally altered nanoparticles, the actual mean equivalent radius and the nanoparticle density has not been examined. It has been shown, however, that due to the high temperature of the nanoparticles during laser assisted growth, coalescence and eventually desorption of atoms occur. Because coalescence is the dominating process, the actual mean equivalent radius of the laser-tailored nanoparticles is larger than $\langle R_{eq} \rangle = 18$ nm, while the nanoparticle density is less than $n_p = (1.0 \pm 0.1) \times 10^{11}$ cm^{-2}, although approximately the same amount of atoms have been deposited. The same holds also for the thermally altered nanoparticles, but compared to the nanoparticle ensemble prepared by natural growth, the differences are small.

The extinction spectra of samples A1 to A3 are displayed in Fig. 2. As expected, the SPR of the naturally grown nanoparticles (sample A1) is relatively broad and located at approximately 850 nm. In contrast, the position of the SPR of the tailored sample A2 is significantly closer to the excitation wavelength for the SERS measurements, but its extinction amplitude is less, compared to the SPR of sample A1. The extinction spectrum for the thermally altered sample A3 is located at the same position as for sample A2, but its extinction amplitude is slightly higher compared to the SPR of the naturally grown nanoparticles of sample A1.

To verify the expected enhancement due to the laser tailored substrate, SERS spectra of pyrene have been obtained with samples A1 to A3 (Fig. 3). The spectra are dominated by a double peak of sapphire at about 1050 cm^{-1} due to the dielectric support, and a strong background signal is observed due to graphite formation. Nevertheless, subtracting the background, the improvement due to the laser tailoring is clearly visible. The peak hight at 1238 cm^{-1} obtained with sample A2 is twice as high as compared to the SERS spectrum obtained with sample A1 and the signal-to-noise ratio is clearly improved.

Another result is interesting. Although the extinction amplitude of sample A2 is clearly lower as compared to sample A3, the obtained SERS intensity and the signal-to-noise ratio is significantly enhanced, although the SPR position of both samples coincide.

4.2 Excitation wavelength $\lambda = 785$ nm

In order to avoid graphite formation, similar experiments as in Sect. 4.1 have been performed with an excitation

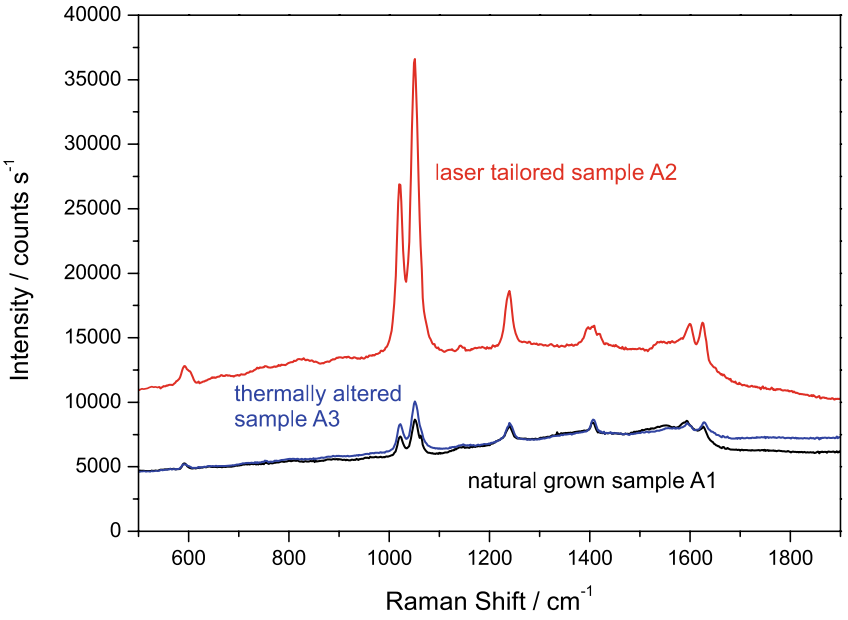

Fig. 3 SERS spectra of pyrene obtained with samples A1 to A3

Table 2 Preparation parameters and characteristics of the SERS substrates B1 and B2 for an excitation with $\lambda = 785$ nm

	B1	**B2**
$\Theta/10^{16}$ cm^{-2}	8 ± 1	8 ± 1
$T_{\text{support}}/\ 10^2$ K	3.0 ± 0.2	3.0 ± 0.2
$\langle a/b \rangle_{\text{eff}}$	0.05	0.07
λ_{SPR}/ nm	>1000	850

wavelength of $\lambda = 785$ nm. For this second set of experiments, two samples (B1 and B2) were prepared. While the nanoparticles of sample B1 were naturally grown, sample B2 was prepared by laser-assisted growth ($h\nu = 1.15$ eV, $F = 40$ mJ/cm^2) in order to optimize the SPR in the vicinity of the excitation wavelength of $\lambda = 785$ nm. The preparation parameters and sample characteristics are summarized in Table 2. The mean radius of the nanoparticles and the nanoparticle density for the ensemble prepared in natural growth have been set again to $\langle R_{\text{eq}} \rangle = (18 \pm 3)$ nm and $n_p = (1.0 \pm 0.1) \times 10^{11}$ cm^{-2}. Hereafter, samples B1 and B2 are called naturally grown and laser-tailored, respectively. The extinction spectra of both samples are displayed in Fig. 4. Again, due to the tailoring, the center position of the SPR of the optimized nanoparticles ($\lambda_{\text{SPR}} = 850$ nm) is closer to the excitation wavelength for the SERS measurements compared to the position of the SPR of the naturally grown nanoparticles, which is well above $\lambda_{\text{SPR}} = 1000$ nm. As a result, an enhanced SERS signal is expected for the tailored nanoparticles compared to the naturally grown nanoparticles.

As in Sect. 4.1, the enhancement due to the tailoring has been verified by obtaining SERS spectra of pyrene. The results are displayed in Fig. 5. Although the differences in the optical properties were small, the SERS spectra obtained with the tailored nanoparticles show a 40% higher signal-to-noise ratio compared to the spectra obtained with naturally grown nanoparticles. Furthermore, nearly no background can be observed, demonstrating that the molecules did not decompose during the measurements.

5 Discussion

5.1 General remarks

The first remarkable observation is that SERS activity of all samples has been detected, i.e., the main peaks of pyrene were always observed. The lack of reproducibility, a drawback of many other kinds of SERS substrates [6], is not seen here, i.e., for the SERS substrates investigated in this work. For this reason, the preparation method is found highly suitable for the production of reproducible SERS substrates.

We emphasize another important finding. The substrates did not show degradation during the measurements, allowing stable signals for long periods of time. The substrates turn out to be so robust that they could be reused. The high stability is a result of the preparation process. The contact area between the oblate nanoparticles and the substrate is large, compared to spherical nanoparticles prepared in solution and subsequently deposited. The larger contact area results in a better binding of the nanoparticles on the substrate, which is thought to be the reason for the high stability of the nanoparticles during the SERS measurements. The high stability of our substrates contrasts other classes

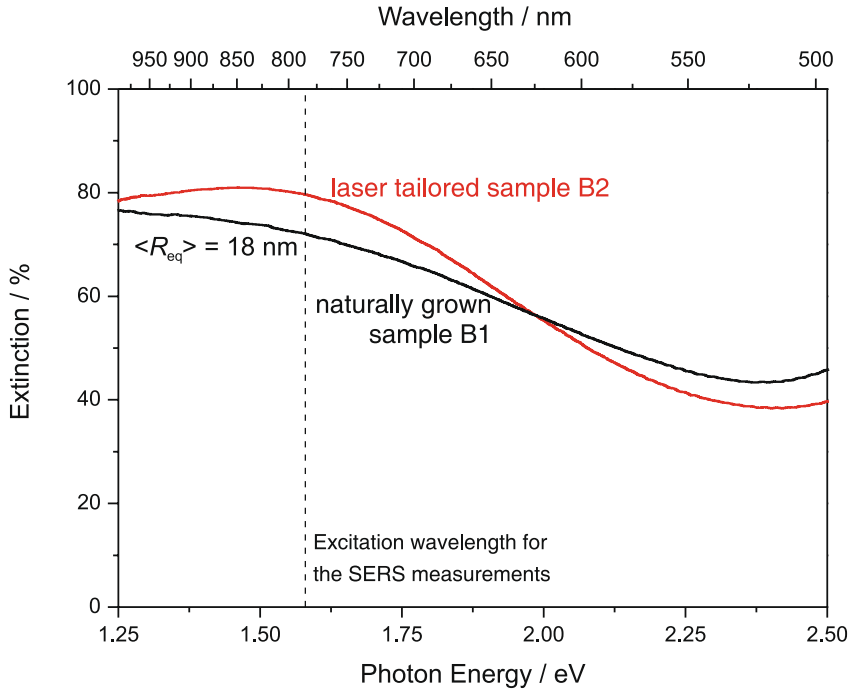

Fig. 4 Extinction spectra of samples B1 and B2

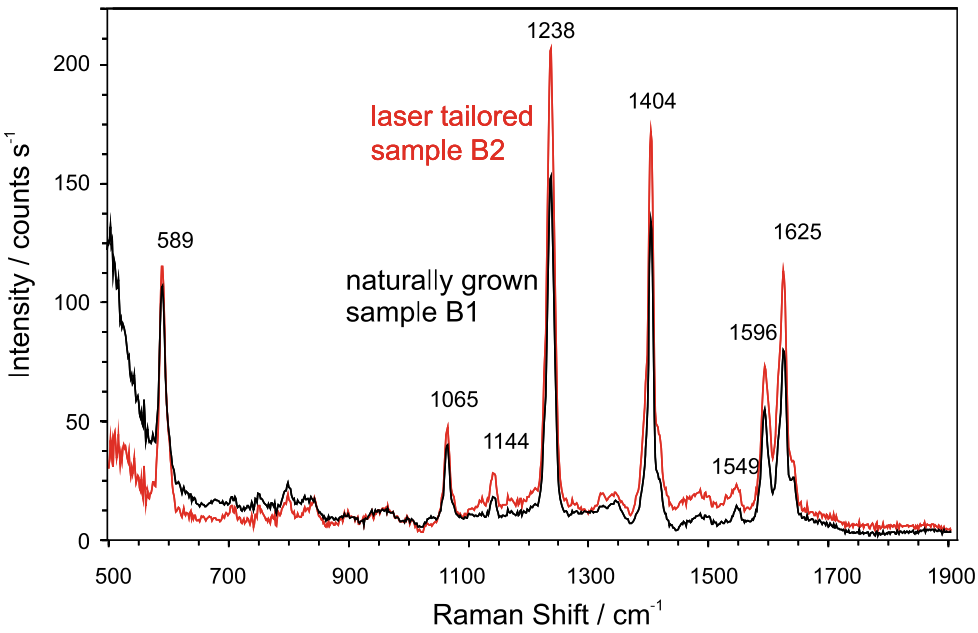

Fig. 5 SERS spectra of pyrene obtained with samples B1 and B2

of SERS substrates, which show strong SERS signals only during a relatively short period of time [1].

The enhancement factors of the SERS substrates were calculated as the ratio of the measured SERS intensity divided by the Raman intensity, which both are normalized to the number of scattering molecules in the focal volume. Since a spot of the pyrene solution disposed on an uncoated substrate yields no measurable Raman intensity under the same measuring conditions, even when increasing the integration time, a 50 mM pyrene solution in methanol measured in a liquid cell served as reference. The quantity of pyrene in the focus of a substrate was estimated to be 5 pico mole and assuming uniform dispersion of the analyte molecules across the spot area, enhancement factors of the order of 10^5 to 10^6 were calculated for the substrates. This value is the average of the area probed by the laser and for the substrate. The exact distribution of the analyte is not known, but measurements across the spotted area have shown that the coverage of the analyte on the substrate tends to be higher at the borders of the liquid spot.

5.2 Influence of laser tailoring

In both sets of experiments described above, a clear improvement of the signal-to-noise ratio due to the tailoring has been realized. The reason is twofold. First, the tailored nanoparticle ensembles have a smaller shape distribution as compared to the naturally grown nanoparticle ensembles. Second, the peak of the surface plasmon resonance of the laser-tailored substrates is closer to the excitation wavelength of the laser light. Both effects mean that significantly more nanoparticles are in resonance with the excitation wavelength for the SERS measurements, and, consequently, more molecules can be excited.

Furthermore, the signal-to-noise ratio of the tailored nanoparticles is even better than that of the thermally altered nanoparticles, although the ensemble shows a significantly lower extinction at the excitation wavelength for the SERS measurements. The lower extinction can be explained mainly by the reduced nanoparticle density and, to a certain extent, by desorption of gold atoms. Both effects are well known in laser tailoring experiments [21, 22, 37]. The better signal-to-noise ratio is due to the mechanisms of laser-assisted growth. With this method, only large nanoparticles with axial ratios smaller than required are tailored [21, 22, 35]. Smaller nanoparticles with higher axial ratio remain uneffected by the laser light. In contrast, tuning the SPR of nanoparticles with elevated temperatures causes a shape change of all nanoparticles towards more spherical. At the end, only few large nanoparticles in an ensemble have the required axial ratio. Thus, the number of nanoparticles in resonance with the excitation wavelength for SERS is significantly less in the thermally altered ensemble as compared to the ensemble tailored with laser light.

5.3 Advantages of laser assisted growth

The main advantage of laser-assisted growth is that, in principle, the position of the SPR can be located at any predetermined photon energy. Thus, the optical properties of the nanoparticles can be optimized for any given SERS excitation wavelength/molecule combination. For example, for molecules such as pyrene, which decompose under irradiation with energetic laser light, SERS excitation with low photon energies is necessary. Laser-assisted growth allows us to stabilize the SPR also at low photon energies, as demonstrated in Sect. 4.2.

Furthermore, due to the tailoring process, the size and shape distribution of the nanoparticles is narrowed, and more nanoparticles are in resonance with the SERS excitation wavelength compared to naturally grown or thermally altered nanoparticles. This results in an overall higher field enhancement at the excitation wavelength for the SERS measurements.

6 Conclusion

In this contribution, we have demonstrated that optimized nanoparticle ensembles prepared by laser-assisted growth on dielectric supports are ideal substrates for surface-enhanced Raman spectroscopy. Tailoring the optical properties of the nanoparticles, i.e., optimizing the SPR within the Stokes and anti-Stokes ranges, has been achieved by irradiating the nanoparticles during growth with ns-pulsed laser light. The signal-to-noise ratio of the SERS signals obtained from the tailored nanoparticles was up to two times higher compared to the signal-to-noise ratio of naturally grown nanoparticles. Furthermore, for the measurements with an excitation wavelength of $\lambda = 785$ nm, a decomposition of the pyrene and, thus, graphite formation is avoided. The determined enhancement factor for the SERS signals obtained from the tailored nanoparticles is in the order of 10^5 to 10^6, i.e., the nanoparticles are good amplifiers.

In addition, a comparison between the SERS signals obtained with tailored nanoparticles to those obtained from thermally altered nanoparticles has been performed. The results show that the tailored nanoparticles are even better than the thermally altered nanoparticles, although the latter ones exhibit a higher extinction amplitude at the excitation wavelength for the SERS measurements.

Another important result was that all substrates were SERS active and posses high stability, an advantage often not found for substrates made by other methods. In combination with the high reproducibility, laser-assisted growth is a versatile method to prepare optimized substrates for surface-enhanced spectroscopies. It is reliable, easy to apply, and generates nanoparticle ensembles with high enhancement factors, making them good candidates not only as optimized substrates for routine use but also to study the influence of the nanoparticle morphology on the electromagnetic enhancement.

Acknowledgements Financial support by the Deutsche Forschungsgemeinschaft (SPP 1093) and of the European Commission under contract HPRN-CT-2002-00328 NANOCLUSTER is gratefully acknowledged.

References

1. S. Nie, S.R. Emroy, Science **275**, 1102 (1997)
2. K. Kneipp, Y. Wang, H. Kneipp, L.T. Perelman, I. Itzkan, R.R. Dasari, M.S. Feld, Phys. Rev. Lett. **78**, 1667 (1997)
3. T. Murphy, H. Schmidt, H.-D. Kronfeldt, Appl. Phys. B **69**, 147 (1999)
4. T. Murphy, S. Lucht, H. Schmidt, H.-D. Kronfeldt, J. Raman Spectrosc. **31**, 943 (2000)
5. S. Lucht, T. Murphy, H. Schmidt, H.-D. Kronfeldt, J. Raman Spectrosc. **31**, 1017 (2000)
6. A. Kudelski, B. Pettinger, Chem. Phys. Lett. **383**, 76 (2004)
7. A. Otto, J. Raman Spectrosc. **33**, 593 (2002)

8. M. Fleischmann, P.J. Hendra, A.J. McQuillan, Chem. Phys. Lett. **2**, 163 (1974)
9. M.G. Albrecht, J.A. Creighton, J. Am. Chem. Soc. **99**, 5215 (1977)
10. J. Lakowicz, B. Shen, Z. Gryczynski, S. D'Auria, I. Gryczynski, Biochem. Biophys. Res. Commun. **286**, 875 (2001)
11. J. Lakowicz, B. Shen, S. D'Auria, J. Malicka, J. Fang, Z. Gryczynski, I. Gryczynski, Anal. Biochem. **301**, 261 (2002)
12. M. Alschinger, M. Maniak, F. Stietz, T. Vartanyan, F. Träger, Appl. Phys. B **76**, 771 (2003)
13. M. Moskovits, L.-L. Tay, J. Yang, T. Haslett, SERS and the single molecule, in *Topics of Applied Physics*, ed. by V.M. Shalaev. Optical Properties of Nanostructured Random Media, vol. 82 (Springer, Berlin, 2002)
14. K. Kneipp, H. Kneipp, I. Itzkan, R.R. Dasari, M.S. Feld, J. Phys., Condens. Matter. **14**, R597 (2002)
15. K. Kneipp, H. Kneipp, I. Itzkan, R.R. Dasari, M.S. Feld, Chem. Rev. **99**, 2957 (1999)
16. K. Li, X. Li, M.I. Stockman, D.J. Bergman, Phys. Rev. B **71**, 115409 (2005)
17. Z.J. Wang, S.L. Pan, T.D. Krauss, H. Du, L.J. Rothberg, Proc. Natl. Acad. Sci. USA **100**, 8638 (2003)
18. N. Felidj, S.L. Truong, J. Aubard, G. Levi, J.R. Krenn, A. Hohenau, A. Leitner, F.R. Aussenegg, J. Chem. Phys. **120**, 7141 (2004)
19. C.L. Haynes, A.D. McFarland, M.T. Smith, J.C. Hulteen, R.P. Van Duyne, J. Chem. Phys. B **106**, 1898 (2002)
20. A. Otto, Light scattering in solids IV, in *Electronic Scattering, Spin Effects, SERS and Morphic Effects*, ed. by M. Cardona, G. Guntherodt (Springer, Berlin, 1984)
21. H. Ouacha, C. Hendrich, F. Hubenthal, F. Träger, Appl. Phys. B **81**, 663 (2005)
22. F. Hubenthal, C. Hendrich, H. Ouacha, D. Blázquez Sánchez, F. Träger, Int. J. Mod. Phys. B **19**, 2604 (2005)
23. D. Blázquez Sánchez, F. Hubenthal, F. Träger, J. Phys., Conf. Ser. **59**, 240 (2007)
24. R. Morarescu, D. Blázquez Sánchez, N. Borg, T. Vartanyan, F. Hubenthal, F. Träger, Appl. Surf. Sci. (2009, accepted)
25. T. Wenzel, J. Bosbach, A. Goldmann, F. Stietz, F. Träger, Appl. Phys. B **69**, 513 (1999)
26. M. Volmer, A. Weber, Z. Phys. Chem. **119**, 277 (1925)
27. F. Stietz, J. Bosbach, T. Wenzel, T. Vartanyan, A. Goldmann, F. Träger, Phys. Rev. Lett. **84**, 5644 (2000)
28. J. Bosbach, D. Martin, F. Stietz, T. Wenzel, F. Träger, Appl. Phys. Lett. **74**, 2605 (1999)
29. T. Ziegler, C. Hendrich, F. Hubenthal, T. Vartanyan, F. Träger, Chem. Phys. Lett. **386**, 319 (2004)
30. C. Hendrich, J. Bosbach, F. Stietz, F. Hubenthal, F. Träger, Appl. Phys. B **76**, 869 (2003)
31. F. Hubenthal, T. Ziegler, C. Hendrich, T. Vartanyan, F. Träger, Proc. SPIE **5221**, 29 (2003)
32. U. Kreibig, M. Vollmer, *Optical Properties of Metal Clusters* (Springer, Berlin, 1995)
33. C.F. Bohren, D.R. Huffman, *Absorption and Scattering of Light by Small Particles* (Wiley, Orlando, 1985)
34. T. Yamaguchi, S. Yoshida, A. Kinbara, Thin Solid Films **21**, 173 (1974)
35. F. Hubenthal, M. Alschinger, M. Bauer, D. Blázquez Sánchez, N. Borg, M. Brezeanu, R. Frese, C. Hendrich, B. Krohn, M. Aeschlimann, F. Träger, Proc. SPIE **5838**, 224 (2005)
36. C. Hendrich, PhD Thesis, Universität Kassel (2004)
37. V. Resta, J. Siegel, J. Bonse, J. Gonzalo, C.N. Afonso, E. Piscopiello, G. Van Tenedeloo, J. Appl. Phys. **100**, 084311 (2006)